atoms

MDPI

Article

Ionization Cross Sections in the Collision between Two Ground State Hydrogen Atoms at Low Energies

Saed J. Al Atawneh [1], Örs Asztalos [2], Borbála Szondy [2], Gergő I. Pokol [2,3] and Károly Tőkési [1,*]

1 Institute for Nuclear Research, ATOMKI, 4032 Debrecen, Hungary; saed.al-atawneh@atomki.mta.hu
2 Institute of Nuclear Techniques, Budapest University of Technology and Economics, Műegyetem rkp. 3, 1111 Budapest, Hungary; asztalos@reak.bme.hu (Ö.A.); szondy.borbala@reak.bme.hu (B.S.); pokol@reak.bme.hu (G.I.P.)
3 Centre for Energy Research, Konkoly-Thege Miklos 29-33, 1121 Budapest, Hungary
* Correspondence: tokesi@atomki.mta.hu

Received: 10 May 2020; Accepted: 17 June 2020; Published: 22 June 2020

Abstract: The interaction between two ground state hydrogen atoms in a collision was studied using the four-body classical trajectory Monte Carlo method. We present the total cross sections for the dominant channels, namely for the single ionization of the target, the ionization of the projectile, resulting from pure ionization, and also from the electron transfer (capture or loss) processes. We also present cross sections for the complete break of the system, resulting in the final channel for four free particles. The calculations were carried out at low energies, relevant to the interest of fusion research. We present our cross sections in the projectile energy range between 2.0 keV and 100 keV and compare them with previously obtained theoretical and experimental results.

Keywords: classical trajectory Monte Carlo method; ionization; four-body collision

1. Introduction

Beam emission spectroscopy (BES) is an active plasma diagnostic tool used for density measurements in fusion research [1]. In this technique, a high energy neutral beam of 2.0–100 keV, composed of typically hydrogen atom, light alkali atoms or their isotopes, is injected into the plasma. Through collisional processes with plasma particles, the beam atoms are excited and, subsequently, spontaneous transitions occur, emitting light, which can be observed. Fluctuations in light emission contribute significantly to the study of plasma density fluctuation and related flows. BES codes, modelling the expected light emission from input plasma parameters, require cross section data, such as collisional excitation, de-excitation, charge exchange, and ionization cross sections [2]. Recent plasma research has shifted the focus on the impact of neutrals located at the plasma edge [3], emphasizing the neutral–neutral collision cross sections, where we have limited data for most of the impact energies or suffer from a lack of cross sections.

The classical trajectory Monte Carlo (CTMC) method is largely employed in collision physics from low to high projectile energies to determine excitation, charge exchange, and ionization cross sections [4]. The CTMC method has been successful in dealing with the ionization processes in ion–atom collisions [5–13]. One of its main advantages is that all interactions among the particles can be taken into account exactly during the collision within the framework of the classical dynamics. The model is based on the numerical integration of the classical equations of motions for the investigated system.

For the case of the collision between two hydrogen atoms, all of the interactions can be exactly taken into account [13]. Here we can take advantage of the classical treatment that, in principle, we do not have any theoretical limit for the number of particles. We can follow all particle trajectories during the collision with the restriction of the classical dynamics. In our previous work, a four-body

classical trajectory Monte Carlo method was utilized to calculate the doubly-differential cross section of projectile ionization at forward observation angles in the H + H collision system at an impact energy of 70 keV/amu. We presented a simple and fast procedure, based on the separation of the interaction regions, for determining the electron loss to the continuum peak with neutral projectiles.

In this work, we present a comparative study between atomic collision calculation methods, such as the classical trajectory Monte Carlo method, convergent close coupling (CCC) approach, semi-quantal method, and Born method, in collisions between two ground state hydrogen atoms. The theoretical results are also compared with the experimental data.

2. Theory

In our model, the four particles (target nucleus, target electron, projectile electron, and projectile nucleus) are characterized by their masses and charges. The projectile nucleus is denoted by P, the projectile electron by P_e, the target nucleus by T and the target electron by T_e. The electron–electron interaction is explicitly included in our four-body calculation. At the time t= – ∞ , we consider four particles as two separate atoms, consisting of the projectile system (P, P_e) labelled as particles (1, 2), and the target system (T, T_e) labelled as particles (3, 4), as shown in Figure 1. Initially, both the projectile (P, P_e) and the target (T, T_e) are in the ground state. We utilize Coulomb potential [4] for describing all interactions. Figure 1 shows the relative position vectors of the four-body collision system.

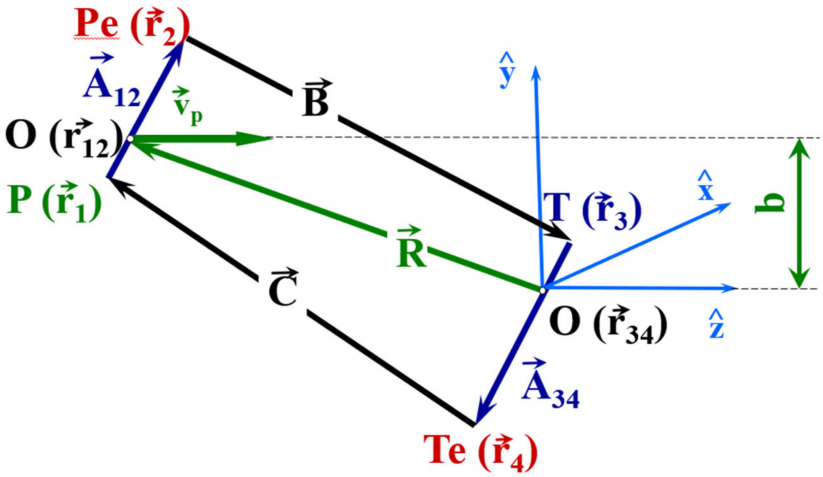

Figure 1. The relative position vectors of the particles involved in four-body collisions.

In the present CTMC simulations, Newton's classical nonrelativistic equations of motion for the four-body system are solved numerically for a statistically large number of trajectories with initial conditions determined pseudorandomly. The Newton equations for the four-body system can be written as:

$$m_i \frac{dr_i^2}{dt^2} = \sum_{i \neq j} Z_i Z_j \frac{|r_i - r_j|}{|r_i - r_j|^3} \quad (i\,,\ j = 1,2,3,4), \tag{1}$$

where m_i, r_i, and Z_i denote the mass, the position vector, and the charge of the ith particle, respectively. The uniform motion of the center of mass of four particles is usually separated out, and the relative motion of the four particles is expressed in terms of their relative positions $A_{34} = r_4 - r_3$, $A_{12} = r_1 - r_2$, $B = r_3 - r_2$, $C = r_1 - r_4$, as shown in Figure 1, and the corresponding velocities $V_{34} = \dot{A}_{34}$, $V_{12} = \dot{A}_{12}$, $V_B = \dot{B}$, $V_C = \dot{C}$. Here, the dot means the derivative with respect to the time variable. From the relation among the relative coordinates:

$$A_{12} + A_{34} + B + C = 0, \tag{2}$$

only three vector equations of motion are independent:

$$\dot{V}_{A12} = \alpha_1 A_{12} + \beta_1 A_{34} + \gamma_1 B, \tag{3}$$

$$\dot{V}_{A34} = \alpha_2 A_{12} + \beta_2 A_{34} + \gamma_2 B, \tag{4}$$

$$\dot{V}_{B} = \alpha_3 A_{12} + \beta_3 A_{34} + \gamma_3 B, \tag{5}$$

where

$$\alpha_1 = \frac{N_1 Z_1 Z_4}{|A_{12} + A_{34} + B|^3} + \frac{N_2 Z_2 Z_4}{|A_{34} + B|^3},$$

$$\beta_1 = \frac{N_1 Z_1 Z_4}{|A_{12} + A_{34} + B|^3} + \frac{(N_1 + N_2) Z_1 Z_2}{A_{12}^3} + \frac{N_1 Z_1 Z_3}{|A_{12} + B|^3},$$

$$\gamma_1 = \frac{N_1 Z_1 Z_4}{|A_{12} + A_{34} + B|^3} - \frac{N_2 Z_1 Z_4}{|A_{34} + B|^3} - \frac{N_2 Z_2 Z_3}{B^3} + \frac{N_1 Z_1 Z_3}{|A_{12} + B|^3} + \frac{N_3 Z_2 Z_3}{B^3},$$

$$\alpha_2 = \frac{N_4 Z_1 Z_4}{|A_{12} + A_{34} + B|^3} + \frac{(N_3 + N_4) Z_3 Z_4}{A_{34}^3} + \frac{N_4 Z_2 Z_4}{|A_{34} + B|^3},$$

$$\beta_2 = \frac{N_4 Z_1 Z_4}{|A_{12} + A_{34} + B|^3} - \frac{N_3 Z_1 Z_3}{|A_{12} + B|^3},$$

$$\gamma_2 = \frac{N_4 Z_1 Z_4}{|A_{12} + A_{34} + B|^3} + \frac{N_4 Z_2 Z_4}{|A_{34} + B|^3} - \frac{N_3 Z_1 Z_3}{|A_{12} + B|^3} + \frac{N_3 Z_2 Z_3}{B^3},$$

$$\alpha_3 = \frac{N_2 Z_2 Z_4}{|A_{34} + B|^3} - \frac{N_3 Z_3 Z_4}{A_{34}^3},$$

$$\beta_3 = \frac{N_3 Z_1 Z_3}{|A_{12} + B|^3} - \frac{N_2 Z_1 Z_2}{A_{12}^3},$$

$$\gamma_3 = \frac{N_3 Z_1 Z_3}{|A_{12} + B|^3} + \frac{(N_2 + N_3) Z_2 Z_3}{B^3} + \frac{N_2 Z_2 Z_4}{|A_{34} + B|^3},$$

$$N_i = (m_i)^{-1} \quad (i = 1, 2, 3, 4).$$

The initial conditions are chosen randomly, at relatively large internuclear distances between the projectile and target atoms (R, in Figure 1), from an ensemble approximating the quantum mechanical phase space distribution for two separate atoms. After numerically integrating to large distances from the collision center, we consider the final exit channels. In this work, we concentrate on the ionization cross sections for both projectile and target. Large numbers of trials were required for reducing the uncertainty of the simulations. The total ionization cross section was computed with the following formula:

$$\sigma = \frac{2\pi b_{max}}{T_N} \sum_{j=1}^{T_N^{(c)}} b_j^{(c)}. \tag{6}$$

The statistical uncertainty of the cross section is given by:

$$\Delta\sigma = \sigma \left[\frac{T_N - T_N^{(c)}}{T_N T_N^{(c)}} \right]^{1/2}. \tag{7}$$

In Equations (6) and (7), T_N is the total number of trajectories calculated for impact parameters less than b_{max}, $T_N^{(C)}$ is the number of trajectories that satisfy the criteria for the investigated final channel, and b_j^C is the actual impact parameter for the trajectory, corresponding to the investigated final channel.

3. Results and Discussion

To study the collision between two ground state hydrogen atoms, we performed a classical simulation with an ensemble of 5×10^5 primary trajectories for each energy. In this work, we focused on the investigation of the ionization channels. At first, let us begin with the net projectile single ionization channel, as defined by Equation (8):

$$H(1s) + H(1s) \rightarrow H^+ + H(nlm) + e^- \tag{8}$$

Classically, this channel is a sum of two channels. We can call the first one the *direct ionization of the projectile* channel. This channel originates from a one-step process. Due to the fact that, classically, the particle motions are deterministic and the electrons in the hydrogen atoms are distinguishable, we can define this classical channel as:

$$(H_p^+, e_p^-) + (H_T^+, e_T^-) \rightarrow H_P^+ + (H_T^+, e_T^-) + e_p^- \tag{9}$$

The second possible classical channel, producing the same final particles as defined by Equation (8), originates from the multi-electron interaction in a two-step process. We refer to this as target ionization and, at the same time, one electron capture of a projectile electron to the bound state of the target. We can define this channel as:

$$(H_p^+, e_p^-) + (H_T^+, e_T^-) \rightarrow H_P^+ + (H_T^+, e_p^-) + e_T^- \tag{10}$$

Figure 2 shows our total cross sections of the single electron loss of the projectile as a function of impact energy in comparison with the calculation of Bailey, et al. [14], and with the experimental data of Wittkower, et al. [15] and McClure [16]. Bailey et al. used a single-center convergent close coupling (CCC) approach for the calculation of one-electron processes and the first Born approximation for the calculation of two-electron processes (B2e). Hereafter we refer this approximation as the CCC+B2e approach. Figure 2 also shows the results of the Born calculations for the total electron-loss cross section (Born EL), as well as the direct ionization cross sections by the CTMC, Born, and single-center CCC results, denoted as CTMC SI, Born SI, and CCC SI, respectively. The CTMC EL provides the best agreement with the experimental data above 20 keV projectile energy. At the same time, in this energy range, the CCC+B2e cross sections are higher than those of the CTMC EL cross sections. On the other hand, at low energies, the CCC+B2e cross sections are very close to the experimental observations. This illustrates the benefit of using a coupled-channel approach. Furthermore, the importance of including the two-electron processes becomes apparent when three models that include one-electron processes only (i.e., CCC SI, CTMC SI, and Born SI) are compared to those that include both one- and two-electron processes (i.e., CCC+B2e EL, CMTC EL, and Born EL). The cross sections obtained with one-electron processes only underestimate the experimental data over the whole energy range considered.

Our collision system is completely symmetric. As a test, we also investigated the net target single ionization channel, defined by Equation (11):

$$H(1s) + H(Is) \rightarrow H(nlm) + H^+ + e^- \tag{11}$$

As for the case of projectile ionization, classically, this channel is also a sum of two channels. We can call the first one the *direct ionization of the target* channel. This channel originates from a one-step process. Due to the fact that, classically, the particle motions are deterministic and the electrons in the hydrogen atoms are distinguishable, we can define this channel as:

$$(H_p^+, e_p^-) + (H_T^+, e_T^-) \rightarrow \ (H_p^+, e_p^-) + H_T^+ + e_T^- \tag{12}$$

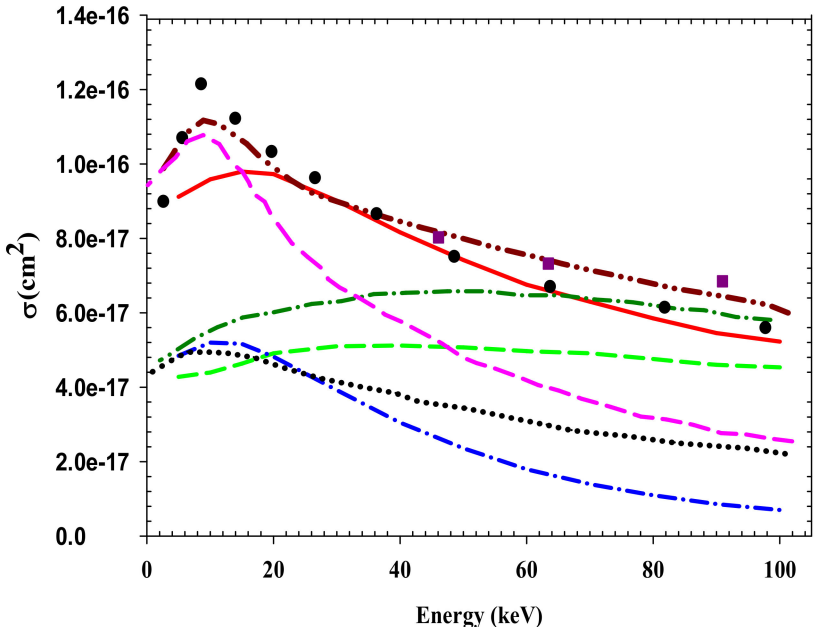

Figure 2. Projectile ionization cross sections in collision between two ground state hydrogen atoms as a function of impact energy. Green dashed line: presents CTMC results for direct ionization (CTMC SI) of the projectile defined by Equation (9). Blue dashed dotted line: presents CTMC results for two-step ionization of projectile defined by Equation (10). Red solid line: projectile ionization cross sections as a result of the sum of the one-step and two-step processes (CTMC EL). Dark brown double-dotted dashed line: the CCC+B2e calculations by Bailey et al. [14]. Dark green dashed dotted line: Born calculations for total electron loss (Born EL). Black dots: Born calculations for single ionization (Born SI). Pink dashed line: CCC calculations for single ionization (CCC SI). Black solid circle: experimental data of McClure [15]. Dark pink square: Experimental data of Wittkower, et al. [16].

The second possible classical channel, producing the same final particles as defined by Equation (11), originates from the multi-electron interaction in a two-step process. We refer to it as projectile ionization and, at the same time, one electron capture of a target electron to the bound state of the projectile. We can define this channel as:

$$(H_p^+, e_p^-) + (H_T^+, e_T^-) \rightarrow (H_p^+, e_T^-) + H_T^+ + e_p^- \tag{13}$$

Figure 3 shows the target ionization cross sections of the ground state hydrogen atom by the hydrogen impact. Figure 3 also shows the previous results of the direct ionization channels by Flannery [17], using the semi-quantal calculation, and by Bates and Griffing [18], using the Born approximation. The present CTMC results for direct target ionization are larger than both the semi-quantal method and the Born method above 30 keV. We note that, according to the expectation, the total cross sections both for the one- and two-step processes for projectile and target ionization are the same.

Last but not least, we calculated the cross sections of the complete break of our system. This reaction channel can be described as:

$$H(1s) + H(Is) \rightarrow H^+ + e^- + H^+ + e^- \tag{14}$$

Figure 4 shows the simultaneous target and projectile ionization cross sections, resulting in the final states four free particles, as a function of the projectile impact. The maximum of the cross sections is around 100 keV.

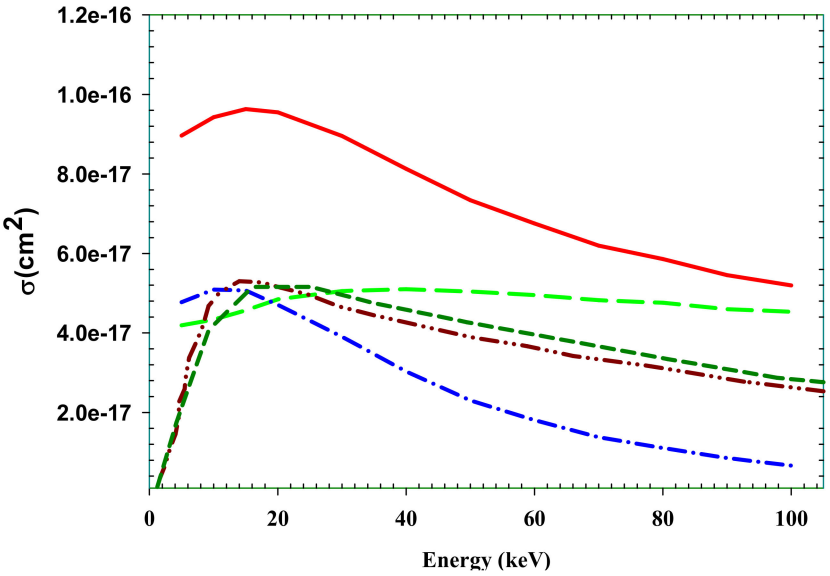

Figure 3. Target ionization cross sections in collision between two ground state hydrogen atoms as a function of impact energy. Green long dashed line: presents CTMC results for direct ionization (CTMC SI) of the target, defined by Equation (12). Blue dashed dotted line: presents CTMC results for two-step ionization of target, defined by Equation (13). Red solid line: target ionization cross sections as a result of the sum of the one-step and two-step processes (CTMC EL). Dark red double-dotted dashed line: semi-quantal calculation for direct ionization of the target by Flannery [17]. Dark green short dashed line: Born calculation for the ionization of the target by Bates and Griffing [18].

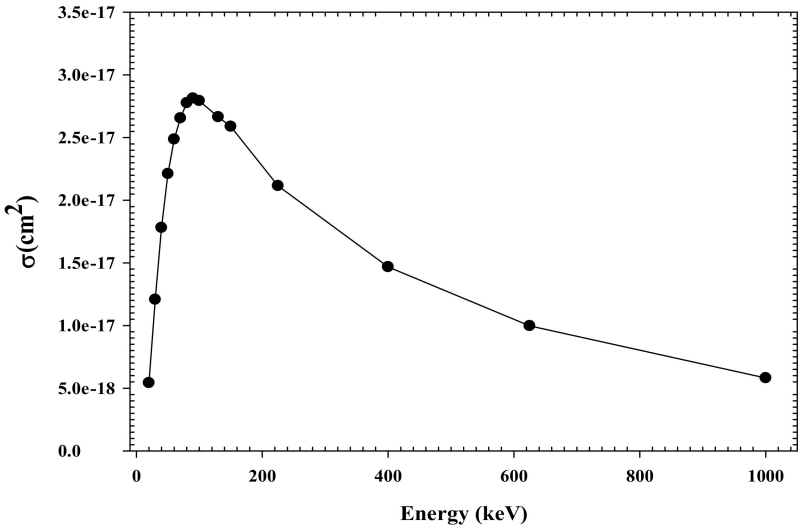

Figure 4. Simultaneous target and projectile ionization cross sections in collision between two ground state hydrogen atoms as a function of projectile impact energy. Filled black circles: present CTMC results.

4. Conclusions

We presented a four-body classical trajectory Monte Carlo simulation of collisions between two ground state hydrogen atoms. The total cross sections for the dominant channels—namely, the net single ionization of the target and ionization of the projectile, resulting from direct ionization and electron transfer (capture or loss) processes for 2.0–100 Kev/amu incident energy of the hydrogen atom impact—have been presented. We also presented cross sections for the complete break of the system, resulting in the final channel for four free particles. While the pure direct ionization channel is a one-step process, the ionization channel in combination with electron capture and loss is a two-step process. Our results were compared with theoretical and experimental data for hydrogen–hydrogen

collision systems with the same energies. Our recent cross sections for projectile ionization (CTMC EL) show excellent and close agreement with the experimental data above 20 keV incident energies and also show good agreement with the CCC+B2e approximation. However, for the case of direct target ionization, our calculated cross sections above 30 keV are higher than the previous theoretical results.

Author Contributions: All authors discussed the results and contributed to the final manuscript. S.J.A.A.: development of CTMC code, performance of analytical and numerical calculations. G.I.P.: has motivated the calculation of the cross-section data for the purposes of beam emission spectroscopy. K.T.: development of CTMC code, performance of analytical calculations and supervised the project. All authors have read and agreed to the published version of the manuscript.

Funding: The work was support by the Hungarian National Research, Development and Innovation Office (NKFIH) Grant Nos: KH126886 and FK132134.

Acknowledgments: The work was supported by the National Research, Development and Innovation Office (NKFIH), Grant KH126886. G. Pokol and O. Asztalos acknowledge the support of the National Research, Development and Innovation Office (NKFIH), Grant FK132134. This work has been carried out within the framework of the EUROfusion Consortium and has received funding from the Euratom research and training programme 2014–2018 and 2019–2020, under grant agreement No 633053. The views and opinions expressed herein do not necessarily reflect those of the European Commission.

Conflicts of Interest: The authors declare no conflict of interest.

References

1. Thomas, D.M.; McKee, G.R.; Burrell, K.H.; Levinton, F.; Foley, E.L.; Fisher, R.K. Chapter 6: Active Spectroscopy. *Fusion Sci. Technol.* **2008**, *53*, 487–527. [CrossRef]
2. Guszejnov, D.; Pokol, G.I.; Pusztai, I.; Refy, D.; Zoletnik, S.; Lampert, M.; Nam, Y.U. Three-dimensional modeling of beam emission spectroscopy measurements in fusion plasmas. *Rev. Sci. Instrum.* **2012**, *83*, 113501. [CrossRef] [PubMed]
3. Wolfrum, E.; Beurskens, M.; Dunne, M.G.; Frassinetti, L.; Gao, X.; Giroud, C.; Hughes, J.; Lunt, T.; Maingi, R.; Osborne, T.; et al. Impact of wall materials and seeding gases on the pedestal and on core plasma performance. *Nucl. Mater. Energy* **2017**, *12*, 18–27. [CrossRef]
4. Tőkési, K.; Hock, G. Versatility of the exit channels in the three-body CTMC method. *Nucl. Instrum. Methods Phys. Res. B* **1994**, *86*, 201–204. [CrossRef]
5. Reinhold, C.O.; Falcon, C.A. Classical ionization and charge-transfer cross sections for H^+ + He and H^+ + Li^+ collisions with consideration of model interactions. *Phys. Rev. A* **1986**, *33*, 3859–3866. [CrossRef] [PubMed]
6. Schultz, D.R.; Olson, R.E. Single-electron–removal processes in collisions of positrons and protons with helium at intermediate velocities. *Phys. Rev. A* **1988**, *38*, 1866–1876. [CrossRef] [PubMed]
7. Schultz, D.R. Comparison of single-electron removal processes in collisions of electrons, positrons, protons, and antiprotons with hydrogen and helium. *Phys. Rev. A* **1989**, *40*, 2330–2334. [CrossRef] [PubMed]
8. Schultz, D.R.; Reinhold, C.O.; Olson, R.E. Large-angle scattering in positron-helium and positron-krypton collisions. *Phys. Rev. A* **1989**, *40*, 4947–4958. [CrossRef] [PubMed]
9. Schultz, D.R.; Meng, L.; Olson, R.E. Classical description and calculation of ionization in collisions of 100 eV electrons and positrons with He and H_2. *J. Phys. B At. Mol. Opt. Phys.* **1992**, *25*, 4601–4618. [CrossRef]
10. Acebal, E.; Otranto, S. Influence of the projectile charge sign in light particle single ionization of H_2O. *Eur. Phys. J. D* **2019**, *73*, 91. [CrossRef]
11. Oliveira, V.; Herbert, A.; Santos, A.; Tőkési, K. Electron capture and loss of O^+ projectile in collision with water near the Bragg Peak Energies. *Eur. Phys. J. D* **2019**, *73*, 146. [CrossRef]
12. Tőkési, K.; DuBois, R.D.; Mukoyama, T. Interaction of positronium with helium atoms—The classical treatment of the 5-body collision system. *Eur. Phys. J. D* **2014**, *68*, 255. [CrossRef]
13. Tökési, K.; Wang, J.; Olson, R.E. Projectile ionization at forward observation angles for intermediate energy H + H collisions. *Nucl. Instrum. Methods Phys. Res. Sect. B Beam Interact. Mater. At.* **1994**, *86*, 147–150. [CrossRef]
14. Bailey, J.J.; Abdurakhmanov, I.B.; Kadyrov, A.S.; Bray, I.; Mukhamedzhanov, A.M. Proton-beam stopping in hydrogen. *Phys. Rev. A* **2019**, *99*, 042701. [CrossRef]
15. McClure, G. Ionization and Electron Transfer in Collisions of Two H Atoms: 1.25–117 keV. *Phys. Rev.* **1968**, *166*, 22–29. [CrossRef]

16. Wittkower, A.B.; Levy, G.; Gilbody, H.B. An experimental study of electron loss during the passage of fast hydrogen atoms through atomic hydrogen. *Proc. Phys. Soc.* **1967**, *91*, 306–309. [CrossRef]
17. Flannery, M. Excitation and Ionization of Hydrogen by Hydrogen-Atom Impact. *J. Phys. B At. Mol. Phys* **1970**, *3*, L97–L100. [CrossRef]
18. Bates, D.R.; Griffing, R.G.W. Inelastic Collisions between Heavy Particles I: Excitation and Ionization of Hydrogen Atoms in Fast Encounters with Protons and with other Hydrogen Atoms. *Proc. Phys. Soc. A* **1953**, *67*, 961–971. [CrossRef]